

## Article

# Many-Objective Hierarchical Pre-Release Flood Operation Rule Considering Forecast Uncertainty

Yongqi Liu <sup>1</sup>, Guibing Hou <sup>1</sup>, Baohua Wang <sup>1</sup>, Yang Xu <sup>2,\*</sup>, Rui Tian <sup>2</sup>, Tao Wang <sup>2</sup> and Hui Qin <sup>3</sup>

<sup>1</sup> China Water Resources Pearl River Planning Surveying & Designing Co., Ltd., Guangzhou 510610, China; yongqil@hust.edu.cn (Y.L.)

<sup>2</sup> Hubei Key Laboratory of Intelligent Yangtze and Hydroelectric Science, China Yangtze Power Co., Ltd., Yichang 443000, China

<sup>3</sup> School of Hydropower and Information Engineering, Huazhong University of Science and Technology, Wuhan 430072, China

\* Correspondence: xy\_mine@sohu.com; Tel.: +86-152-0720-8560

**Abstract:** Flood control operation of cascade reservoirs is an important technology to reduce flood disasters and increase economic benefits. Flood forecast information can help reservoir managers make better use of flood resources and reduce flood risks. In this paper, a hierarchical pre-release flood operation rule considering the flood forecast and its uncertainty information is proposed for real-time flood control. A many-objective optimization model considering the cascade reservoir's power generation objective, flood control objective, and navigation objective is established. Then, a region search evolutionary algorithm is applied to optimize the many-objective optimization model in a real-world case study upstream of the Yangtze River basin. The optimization experimental results show that the region search evolutionary algorithm can balance convergence and diversity well, and the HV value is 40% higher than the MOEA/D algorithm. The simulation flood control results of cascade reservoirs upstream of the Yangtze River demonstrate that the optimized flood control rule can increase the average multi-year power generation of cascade reservoirs by a maximum of  $27.72 \times 10^8$  kWh under the condition of flood control safety. The rules proposed in this paper utilize flood resources by identifying runoff forecast information, and pre-release to the flood limit level 145 m before the big flood occurs, so as to ensure the safety downstream and the dam's own flood control and provide reliable decision support for reservoir managers.

**Keywords:** flood control operation; many-objective problem; flood forecasting; inflow uncertainty; two-stage reservoir operation model



**Citation:** Liu, Y.; Hou, G.; Wang, B.; Xu, Y.; Tian, R.; Wang, T.; Qin, H. Many-Objective Hierarchical Pre-Release Flood Operation Rule Considering Forecast Uncertainty.

*Water* **2024**, *16*, 785. <https://doi.org/10.3390/w16050785>

Academic Editor: Giovanni Ravazzani

Received: 1 February 2024

Revised: 29 February 2024

Accepted: 3 March 2024

Published: 6 March 2024



**Copyright:** © 2024 by the authors. Licensee MDPI, Basel, Switzerland. This article is an open access article distributed under the terms and conditions of the Creative Commons Attribution (CC BY) license (<https://creativecommons.org/licenses/by/4.0/>).

## 1. Introduction

Among various hydro-meteorological disasters, floods are one of the most destructive disasters in the world [1], which often cause large numbers of casualties and economic losses [2]. With the development of the social economy, urbanization, and the increase in population, it is anticipated that the occurrence rates and intensity of floods will increase, which may cause more economic losses [3,4]. The construction and development of cascade reservoirs are the main measures to reduce and resist flood disasters, and the operation rules of cascade reservoirs play an important role in real-time flood control [5]. However, most of the early conventional reservoir operation rules, such as operation graph and the design flood control rules [6], only give a simple decision direction (e.g., outflow or output) based on the current reservoir state and do not take into account future forecast scenarios and their uncertain information. Climate change has led to anomalous fluctuations in extreme streamflow from global river systems, and the superposition of human activities such as damming has compounded the changes in extreme streamflow, affecting floods and river ecosystems [7]. Therefore, there is an urgent need to optimize the original

scheduling and operation rules for reservoir clusters so that they can be more adapted to the present environment.

With the development of optimization theory [8,9], more and more researchers have begun to study reservoir optimization operation rules [10,11]. According to the existing literature, there are mainly two approaches for obtaining optimal reservoir operation rules. One approach is to use data mining methods to derive optimal decision rules based on deterministic reservoir optimization operation solutions, such as fuzzy inference systems [12], extreme learning machines [13], and the Bayesian deep learning method [14]. However, these data-to-data-driven methods simply capture the correlations between data, and the parameters of the model have no practical meaning, which may confuse reservoir operation managers. Another approach is to predefine the form of the rules and parameterize them, such as curves or tables, and then optimize the parameters in the rules by optimization algorithms [15]. During the last decades, different kinds of reservoir operation rules and optimization algorithms have been proposed to improve the benefits of reservoir real-time operation and management [16–18]. A multi-objective energy storage operation chart (ESOC) optimization model considering ecological flow was proposed for large-scale mixed reservoirs. Their study showed that the ESOC optimization model was able to determine the multi-objective Pareto fronts of different minimum discharges of upstream reservoirs, which significantly improved the power generation benefit of the traditional reservoir operation chart [19]. A hierarchical flood operation rule (HFOR) and a multi-objective cultured evolutionary algorithm were proposed for flood resource utilization [20], and the experimental results showed that the optimized HFORs could improve power generation under the premise of ensuring flood control safety. An adaptive hybrid differential evolution algorithm was proposed to optimize the operating rules of multi-reservoir hydropower generation systems [21], and the proposed optimization algorithm could generate significantly more hydropower energy.

These studies indicate that we can define a new reservoir operation rule or improve the traditional reservoir operation rule and use optimization algorithms to optimize these rules to improve the objectives of the cascade reservoirs. However, most of these reservoir operation rules lack the consideration of forecasted reservoir inflow and forecasting uncertainty [22]. With the development of computer science, more and more hydrological forecasting models and forecasting uncertainty estimation methods have been proposed [23–26]. To consider inflow forecast information in reservoir operation rules, a two-stage reservoir operation model with hedging rule policies that explicitly includes uncertain future reservoir inflow was proposed [27,28]. In recent years, reservoir hedging rule policies have been applied to various tasks of reservoirs. For example, optimal hedging rules were developed using hydroeconomic and mathematical analyses for reservoir flood control operations [29]. An analytical framework for flood water conservation was proposed to derive hedging rules, which showed how much flood water could be conserved for use after the flood season through the hedging rules [30]. An improved aggregated hedging rule was proposed for a multi-reservoir water-supply system, which could improve both water supply quality and hydropower generation of the multi-reservoir [31]. A two-stage metaheuristic mixed-integer nonlinear programming approach was proposed to extract optimum hedging rules for multi-reservoir systems, which significantly reduced the magnitude of failures during drought periods [32].

Inspired by hedging rule policies and the approach for optimizing reservoir operation rules by optimization algorithms, we propose a many-objective optimization model of a hierarchical pre-release flood control operation rule (HPFOR) that considers inflow forecast uncertainty. The inflow uncertainty is represented by a multi-step daily inflow forecast model [33] with a probabilistic streamflow forecasting method [34]. The HPFOR is optimized by the region search evolutionary algorithm (RSEA) [35]. The innovation of this study is the construction of a hierarchical forecast pre-discharge operation mode considering runoff forecast uncertainty, by a two-stage model and uncertainty analysis, and optimizing the parameters by an evolutionary algorithm, so as to obtain the optimal

operation rules to enhance the comprehensive use efficiency of the basin reservoir cluster. The major contributions are outlined as follows:

- (1) First and foremost, the two-stage reservoir operation model and the impact of forecast uncertainty on the model are analyzed. Then, the HPFOR is defined by multiple flow thresholds under the maximum release flow and sub-pre-release flood operation rules between each flow level.
- (2) Many-objective optimization models of the HPFOR with a power generation objective, flood control objective, and navigation objective are established. Furthermore, a constrained RSEA is applied to solve the many-objective optimization model of HPFOR.
- (3) The comparison of three state-of-the-art algorithms with RSEA is shown to demonstrate the performance of the RSEA. The comparison of conventional flood control rules, HFOR, and HPFOR is shown to prove the advantages of the proposed HPFOR.

The remainder of this paper is organized as follows. In Section 2, the methodology is given in detail, which includes the probabilistic streamflow forecasting model, the proposed HPFOR, the many-objective optimization model, and the RSEA. In Section 3, an application of HPFOR is presented. The conclusions are given in Section 4.

## 2. Methodology

The flowchart of the many-objective hierarchical pre-release flood operation rule considering forecast uncertainty is shown in Figure 1. The details of the methodology and modeling are given in subsequent sections.

### 2.1. Probabilistic Streamflow Forecasting Model

In the real-time reservoir flood control operation during the flood season, future streamflow forecasting and forecasting uncertainty information are of great importance for water resources managers to better utilize small and medium floods and reduce the risk of large floods. Therefore, a probabilistic streamflow forecasting model is needed to give accurate and reliable flood forecast results. Based on our previous work, the directed graph deep neural network (DGDNN) [33] is applied to predict the multi-step daily inflow of a cascade reservoir and hidden Markov regression (HMR) [34] is applied to obtain the probability distribution of the predicted streamflow.

The main idea of the DGDNN is to construct a directed graph structure of meteorological and hydrological stations and then use the spatial information capture process and the feature aggregation process to predict the streamflow of target hydrological stations. The spatial information capture process consists of a multi-convolution layer and a full connect layer, which are used to capture the influence of the rainfall of meteorological stations on the runoff of hydrological stations, which is regarded as a rainfall–runoff model in the hydrological stations. The feature aggregation process is composed of a multi-layer perceptual network for aggregating the captured precipitation information and the streamflow information that affect the target hydrological station, which is regarded as a confluence process in the hydrological station.

After forecasting the multi-step streamflow by the DGDNN, the uncertainties in different forecast periods are given by HMR. In HMR, the observation model is assumed as a joint Gaussian distribution. The joint data  $x$  can be divided into two subvectors  $x = [x^1; x^2]$ , where  $x^1$  denotes the forecasting result of the DGDNN and  $x^2$  denotes the observed streamflow data. Finally, the uncertainty in the forecast streamflow can be quantified as follows:

$$\begin{aligned}
 p(x_t^2 | x_t^1) &= \frac{p(x_t^1, x_t^2)}{p(x_t^1)} \\
 &= \frac{\sum_{k=1}^K \left[ \left( \sum_{i=1}^K h_{t-1}(i) A_{ik} \right) N(x_t^1 | \mu_1^k, \Sigma_{11}^k) N(x_t^2 | \mu_{21}^k, \Sigma_{21}^k) \right]}{\sum_{j=1}^K \left[ \left( \sum_{i=1}^K h_{t-1}(i) A_{ij} \right) N(x_t^1 | \mu_1^j, \Sigma_{11}^j) \right]} \\
 &= \sum_{k=1}^K h_t(k) N(x_t^2 | \mu_{21}^k, \Sigma_{21}^k)
 \end{aligned} \tag{1}$$

$$h_t(k) = \frac{\left( \sum_{i=1}^K h_{t-1}(i) A_{ik} \right) N\left(x_t^1 \mid \mu_1^k, \Sigma_{11}^k\right)}{\sum_{j=1}^K \left[ \left( \sum_{i=1}^K h_{t-1}(i) A_{ij} \right) N\left(x_t^1 \mid \mu_1^j, \Sigma_{11}^j\right) \right]} \quad (2)$$

where  $K$  is the number of states;  $\pi_k$  is the initial probability of state  $k$ ;  $\mu_k$  and  $\Sigma_k$  are the mean vector and covariance matrix of the  $k$ -th joint Gaussian distribution; and  $h_t(k)$  represents the HMM forward variable.

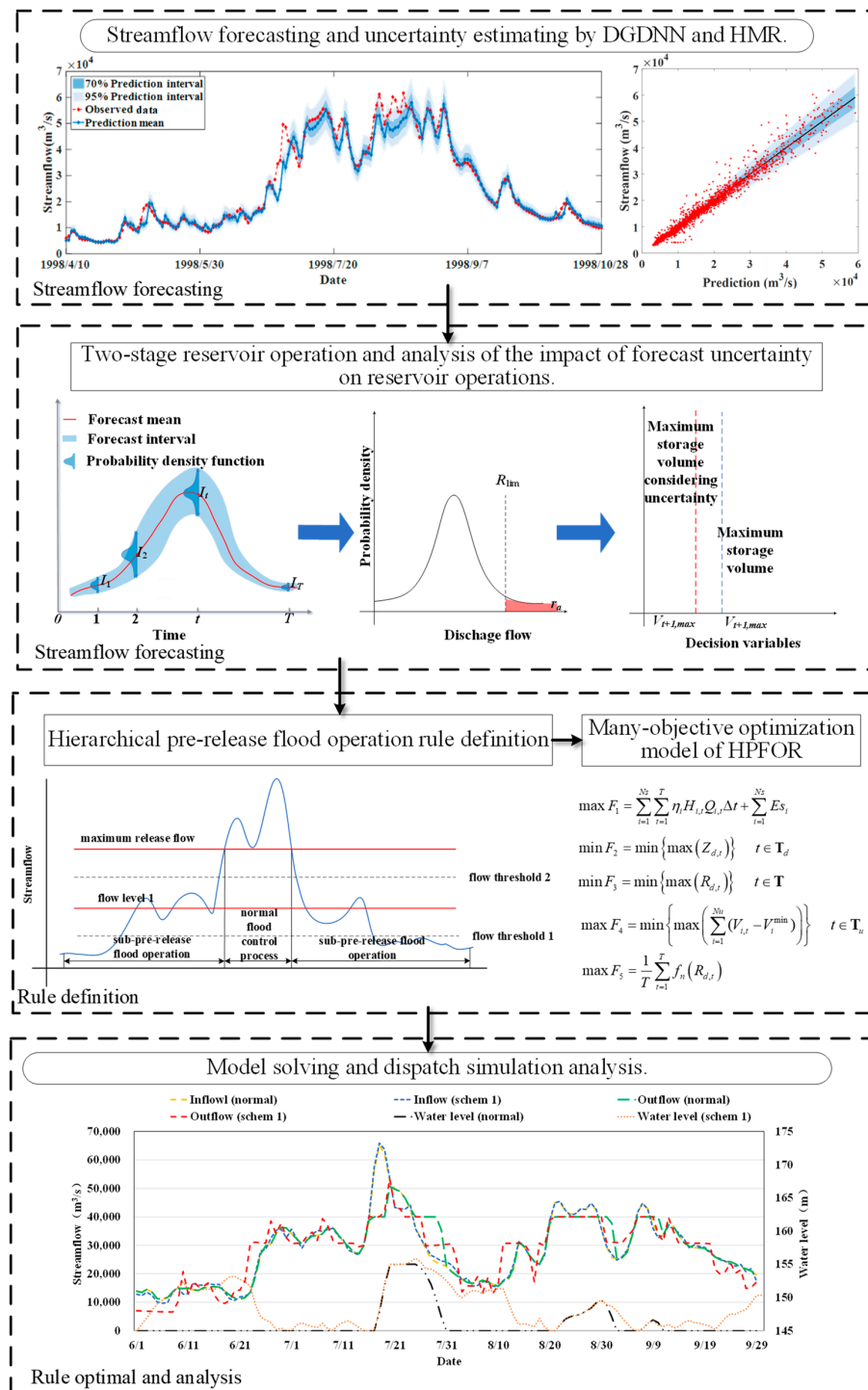


Figure 1. A flowchart of the many-objective hierarchical pre-release flood operation rule considering forecast uncertainty.

According to the uncertainty quantification results, we can obtain the probability density function of the streamflow forecasted by the DGDNN, which can be used in the HPFOR in the next section.

### 2.2. Hierarchical Pre-Release Flood Control Operation Rule

After obtaining the uncertainty in streamflow forecasting, this section mainly introduces the HPFOR based on the two-stage reservoir operation model considering the streamflow forecast uncertainty.

#### 2.2.1. Two-Stage Reservoir Operation Model

In real-time reservoir operation, water resource managers need to make decisions based on the inflow, the storage state of the reservoir, and the streamflow forecast information. When it comes to the next period, the streamflow forecast information will be updated, and the reservoir operation decision will be made again. Therefore, the real-time reservoir operation is a rolling prediction–decision process. The two-stage reservoir operation model divides the rolling prediction–decision process into the following two stages: the first stage is the operation decision-making stage, which only considers the current operation period  $t$ ; the second stage is the forecasting stage, which considers the future  $T_f$  periods according to the streamflow forecasting horizon. The process of the two-stage reservoir dispatch model is shown in Figure 2.

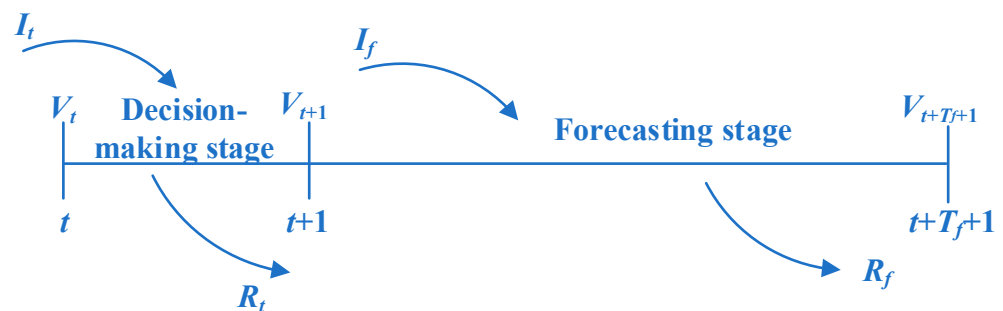


**Figure 2.** The process of the two-stage reservoir dispatch model.

During the flood season, the operation decision-making stage and the forecasting stage in the two-stage reservoir operation model need to meet the following constraints:

- (1) Discharge flow constraint in the decision-making stage:

$$R_t \leq R_{lim} \tag{3}$$

where  $R_t$  is the average discharge flow during the decision-making stage and  $R_{lim}$  is the maximum release flow of the reservoir to ensure the flood control safety of the downstream station.

- (2) Discharge flow constraint in the forecasting stage:

$$R_f \leq R_{lim} \tag{4}$$

where  $R_f$  is the average discharge flow during the forecasting stage.

- (3) Storage volume constraint in the forecasting stage:

$$V_{t+T_f+1} = V_{lim} \tag{5}$$

where  $T_f$  is the forecast horizon of the streamflow forecast,  $V_{t+T_f+1}$  is the storage volume and the end of the forecasting stage, and  $V_{lim}$  is the storage volume corresponding to the flood limit water level of the reservoir.

- (4) Water balance constraint:

$$V_{t+1} = V_t + I_t\Delta t - R_t\Delta t \tag{6}$$

$$V_{t+T_f+1} = V_{t+1} + I_fT_f\Delta t - R_fT_f\Delta t \tag{7}$$

where  $V_t$  is the storage volume at period  $t$ ,  $I_t$  is the average inflow of the reservoir during the decision-making stage,  $I_f$  is the forecast inflow of the reservoir during the forecasting stage, and  $\Delta t$  is the time interval.

By incorporating Formulas (4) and (5) into Formula (7), the inequality of reservoir storage volume in the decision-making stage can be obtained as follows:

$$\begin{aligned} V_{t+1} &= V_{t+T_f+1} - I_fT_f\Delta t + R_fT_f\Delta t \\ &\leq V_{lim} - I_fT_f\Delta t + R_{lim}T_f\Delta t \end{aligned} \tag{8}$$

By incorporating formulas (3) and (8) into formula (6), the inequality of the average discharge flow during the decision-making stage can be obtained as follows:

$$\begin{aligned} R_t &= (V_t + I_t\Delta t - V_{t+1})/\Delta t \\ (V_t - V_{lim})/\Delta t + I_t + I_fT_f - R_{lim}T_f &\leq R_t \leq R_{lim} \end{aligned} \tag{9}$$

### 2.2.2. Impact of Forecast Uncertainty on Reservoir Operation

From the two-stage reservoir operation model, we can see that the decision discharge flow is related to  $I_t$  and  $I_f$ . When considering the uncertainty in the forecast inflow,  $I_f$  is given in the form of probability as follows:

$$I_f \sim p_I(I_f) \tag{10}$$

where  $P_I(I_f)$  denotes the probability density function of the forecast inflow.

With the uncertainty in the forecast inflow, the discharge flow in the forecast stage will also be accompanied by uncertainty. The average discharge flow in the forecast stage obeys the following distribution:

$$R_f \sim p_R(R_f) = (V_{t+1} - V_{lim})/(T_f\Delta t) + p_I(I_f) \tag{11}$$

where  $P_R(R_f)$  denotes the probability density function of the discharge flow.

The discharge flow of the reservoir needs to meet the demands of the downstream flood control station and cannot exceed the maximum discharge flow. Therefore, the uncertainty in the discharge flow will bring risks to the flood control safety. The risk rate can be calculated as follows:

$$r = 1 - p_R(R_{lim}) \tag{12}$$

where  $r$  is the flood control risk and  $P_R(R_{lim})$  denotes the probability that the discharge flow is less than  $R_{lim}$ . According to the hydraulic relationship between the discharge flow and the forecast inflow, the risk rate is converted into the integral form of the probability density function of the inflow forecast as follows:

$$r = 1 - p_I\left(R_{lim} - (V_{t+1} - V_{lim})/(T_f\Delta t)\right) \tag{13}$$

Given a risk rate threshold  $r_a$ , when the risk rate  $r$  is less than or equal to  $r_a$ , it is assumed that the downstream station is in a safe state. Therefore, the following inequality is obtained:

$$\begin{aligned} p_I\left(R_{lim} - (V_{t+1} - V_{lim})/(T_f\Delta t)\right) &\geq 1 - r_a \\ R_{lim} - (V_{t+1} - V_{lim})/(T_f\Delta t) &\geq \text{Per}\left(P_I(I_f), 1 - r_a\right) \end{aligned} \tag{14}$$

where  $\text{Per}\left(P_I(I_f), 1 - r_a\right)$  denotes the  $1 - r_a$  percentile of the forecast streamflow probability  $P_I(I_f)$ .

According to the above inequality, the inequalities of reservoir storage volume and discharge flow considering the uncertainty in inflow forecast can be obtained as follows:

$$V_{t+1} \leq V_{lim} + R_{lim}T_f\Delta t - Per(I_f, 1 - r_a)T_f\Delta t \tag{15}$$

$$(V_t - V_{lim})/\Delta t + I_t + Per(I_f, 1 - r_a)T_f - R_{lim}T_f \leq R_t \leq R_{lim} \tag{16}$$

It can be seen from the inequalities that the risk rate threshold  $r_a$  will affect the decision variables in the decision-making stage as follows: a smaller  $r_a$  will reduce the storage volume of the reservoir and increase the discharge flow; a larger  $r_a$  will increase the storage volume of the reservoir and reduce the discharge flow. In addition, the uncertainty in  $P_I(I_f)$  determines the degree of influence of  $r_a$  on the decision variables: the greater the variance in  $P_I(I_f)$ , the greater the influence of  $r_a$  on the decision variables. The impact of forecast uncertainty on reservoir decisions can be seen in Figure 3.

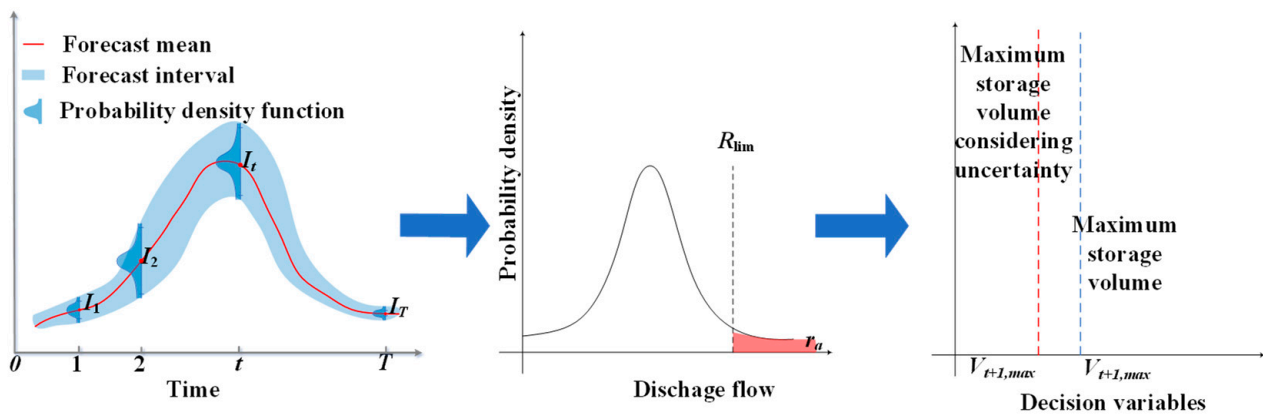


Figure 3. The impact of forecast uncertainty on reservoir decision.

### 2.2.3. Hierarchical Pre-Fill and Pre-Release Strategy

In real-time flood control, the operation process is usually divided into the pre-fill process, the pre-release process, and the normal flood control process [36]. When the forecast inflow is less than the streamflow threshold and the current storage volume is less than the maximum allowable volume of the reservoir, the pre-fill process will be executed. When the forecast inflow is larger than the threshold streamflow and the current inflow is less than the maximum release flow, the pre-release process will be executed. When the current inflow is larger than the maximum release flow, the normal flood control process will be executed.

This paper proposes a hierarchical pre-fill and pre-release strategy in the HPFOR. The main idea of the strategy is to define multiple flow levels and flow thresholds under the maximum release flow and establish hierarchical pre-fill and pre-release rules between each flow level. For example, when there are two flow levels under the maximum release flow, the HPFOR is represented in Figure 4, and the details of the operation rules are as follows:

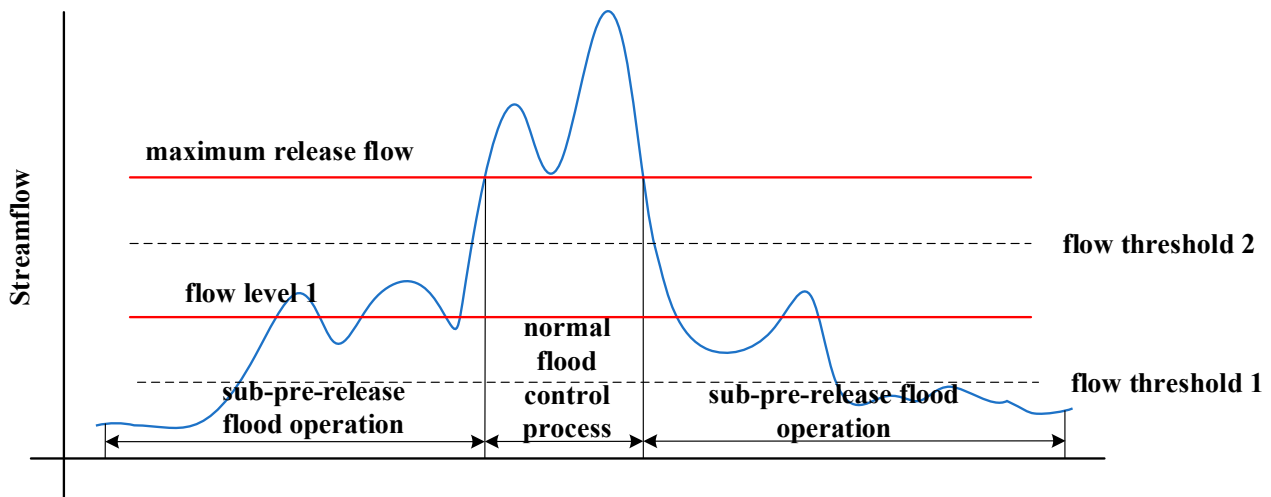


Figure 4. The representation of the HPFOR.

When the forecast inflow is less than flow threshold 1, the pre-fill process will be executed as follows: set flow level 1 as limit flow  $R_{lim}$  and use Formula (15) to calculate the maximum reservoir volume  $V_{max\ t + 1}$  at the end of the decision-making stage. The water level can be raised for water resource utilization.

When the forecast inflow is larger than flow threshold 1 and less than flow level 1, the pre-release process will be executed as follows: set flow level 1 as the release flow and decrease the water level to the flood-limited water level.

When the forecast inflow is larger than flow level 1 and less than flow threshold 2, the pre-fill process will be executed as follows: set maximum release flow as limit flow  $R_{lim}$  and use Formula (15) to calculate the maximum reservoir volume  $V_{max\ t + 1}$  at the end of the decision-making stage. The water level can be raised for water resource utilization.

When the forecast inflow is larger than flow threshold 2 and less than the maximum release flow, the pre-release process will be executed as follows: set the maximum release flow as the release flow and decrease the water level to the flood-limited water level.

When the forecast inflow is larger than flow threshold 2 and the current inflow is larger than the maximum release flow, the normal flood control will be executed as follows: set maximum release flow as the release flow to ensure downstream flood control safety.

### 2.3. Many-Objective Optimization Model of the HPFOR

According to the HPFOR, different flow levels and flow thresholds will form different flood operation rules, and the flow levels and flow thresholds can be set as decision variables in the optimization model. The target of this study is to obtain optimal HPFORs for small and medium floods, which consists of multiple objectives and constraints as follows.

#### 2.3.1. Objective Function

Power generation objective: The power generation objective consists of the total generation of the cascade reservoirs and the total energy storage at the end of the flood season. The formulation is shown as follows:

$$\max F_1 = \sum_{i=1}^{Ns} \sum_{t=1}^T \eta_i H_{i,t} Q_{i,t} \Delta t + \sum_{i=1}^{Ns} E_{s_i} \tag{17}$$

where  $N_s$  is the number of reservoirs;  $T$  is the number of operation periods;  $\eta_i$  is the power production coefficient of the  $i$ -th reservoir;  $\Delta t$  is the operation interval;  $H_{i,t}$  is the water head of  $i$ -th reservoir during the  $t$ -th period;  $Q_{i,t}$  is the release flow passing turbines of the  $i$ -th reservoir during the  $t$ -th period; and  $E_{s_i}$  is the energy storage of the  $i$ -th reservoir at the

end of the flood season, which can be calculated by the available water volume and the average water consumption rate.

Flood control objective of the downstream reservoir: The downstream reservoir flood control objective can be divided into two categories including the safety of the reservoir itself and the flood control station security:

$$\min F_2 = \min \{ \max(Z_{d,t}) \} t \in \mathbf{T}_d \quad (18)$$

$$\min F_3 = \min \{ \max(R_{d,t}) \} t \in \mathbf{T} \quad (19)$$

where  $Z_{d,t}$  is the water level of the downstream reservoir at time  $t$ ;  $\mathbf{T}_d$  is the time set when the reservoir during the flood control process;  $R_{d,t}$  is the release flow of the downstream reservoir at time  $t$ ; and  $\mathbf{T}$  is the time set of the total operation period.

Flood control objective of upstream cascade reservoirs: In the flood control process of cascade reservoirs, the upstream reservoirs can reduce the flood peaks for the downstream reservoir. However, excessive use of upstream flood control storage capacity will increase upstream flood control risks. Therefore, the objective of upstream cascade reservoirs is to minimize the use of flood control storage capacity as follows:

$$\max F_4 = \min \left\{ \max \left( \sum_{i=1}^{Nu} (V_{i,t} - V_i^{\min}) \right) \right\} t \in \mathbf{T}_u \quad (20)$$

where  $Nu$  is the number of upstream cascade reservoirs;  $\mathbf{T}_u$  is the time set when the upstream reservoirs reduce the flood peaks for the downstream reservoir;  $V_{i,t}$  is the storage volume of the  $i$ -th reservoir at time  $t$ ; and  $V_i^{\min}$  is the flood limited water level of the  $i$ -th reservoir.

Navigation objective: In order to improve the navigability of ships during the flood season, the navigation objective is to maximize the navigation rate as follows:

$$\max F_5 = \frac{1}{T} \sum_{t=1}^T f_n(R_{d,t}) \quad (21)$$

where  $f_n(\cdot)$  is the function of the navigation rate, which is related to the release flow  $R_{d,t}$ .

### 2.3.2. Constraints

Water balance constraint:

$$V_{i,t} = V_{i,t-1} + I_{i,t}\Delta t + \sum_{k=1}^{Nu_i} R_{k,t-\tau_{k,i}}\Delta t - R_{i,t}\Delta t \quad (22)$$

where  $V_{i,t}$  is the storage volume of the  $i$ -th reservoir at time  $t$ ;  $I_{i,t}$  is the interval flow of the  $i$ -th reservoir during time period  $t$ ;  $R_{i,t}$  is the release flow of the  $i$ -th reservoir during time period  $t$ ;  $Nu_i$  is the number of reservoirs upstream of the  $i$ -th reservoir; and  $\tau_{k,i}$  is the time delay from reservoir  $k$  to  $i$ .

Reservoir storage volume constraint:

$$V_{i,\min} \leq V_{i,t} \leq V_{i,\max} \quad (23)$$

where  $V_{i,\min}$  and  $V_{i,\max}$  are the lower and upper storage volume limits of the  $i$ -th reservoir.

Release constraint:

$$R_{i,\min} \leq R_{i,t} \leq R_{i,\max} \quad (24)$$

where  $R_{i,\min}$  and  $R_{i,\max}$  are the lower and upper release limits of the  $i$ -th reservoir.

Output constraint:

$$N_{i,\min} \leq \eta_i H_{i,t} Q_{i,t} \Delta t \leq N_{i,\max} \quad (25)$$

where  $N_{i,\min}$  and  $N_{i,\max}$  are the lower and upper output limits of the  $i$ -th reservoir.

#### 2.4. Region Search Evolutionary Algorithm

The proposed optimization model of the HPFOR consists of 5 objectives. According to the definition of the multi-objective optimization problem, when the number of objectives is larger than 3, it is considered as a many-objective optimization problem (MaOP). In order to solve MaOPs, a number of evolutionary multi-objective (EMO) algorithms have been proposed, such as the multi-objective evolutionary algorithm based on decomposition (MOEA/D) [37], the nondominated sorting genetic algorithm III (NSGA-III) [38], the  $\theta$  dominance-based evolutionary algorithm ( $\theta$ -DEA) [39], and the region search evolutionary algorithm (RSEA) [35]. In this paper, a constrained RSEA is applied to solve the many-objective optimization model of the HPFOR. The main idea of the RSEA is to associate each solution with a region and use the region search strategy to constrain the update process, thereby enhancing the diversity of the population without losing convergence. The framework of the RSEA is shown in Algorithm 1, and the details of the RSEA can be seen in our previous work [40].

---

#### Algorithm 1: Framework of the RSEA

---

```

( $\lambda^1, \lambda^2, \dots, \lambda^N$ ) = InitializeWeights()
E = InitializeNeighborhood()
P = InitializePopulation()
 $\mathbf{z}^*$  = InitializeIdealPoint(P)
 $\mathbf{z}^{nad}$  = InitializeNadirPoint(P)
while termination criteria is not satisfied do
  for each subproblem  $i = 1, 2, \dots, N$  do
     $\mathbf{x}^c$  = Reproduction(MP) //  $\mathbf{x}^c$  is an offspring
     $\mathbf{z}^*$  = UpdateIdealPoint( $\mathbf{x}^c$ )
     $\mathbf{z}^{nad}$  = UpdateNadirPoint( $\mathbf{x}^c$ )
    Normalize(P,  $\mathbf{x}^c$ ,  $\mathbf{z}^*$ ,  $\mathbf{z}^{nad}$ )
    P = UpdatePopulation(MP,  $\mathbf{x}^c$ )
  end for
end while

```

---

### 3. Case Study

#### 3.1. Study Area

To verify the advantages of the proposed HPFOR, the Xiluodu, Xiangjiaba, and Three Gorges cascade reservoirs in the Yangtze River are selected as the research areas. The locations of the Xiluodu, Xiangjiaba, and Three Gorges cascade reservoirs are shown in Figure 5. The Xiluodu Hydropower Station is located in the Jinsha River gorge at the junction of the Sichuan and Yunnan Provinces, the catchment area of Xiluodu is 454,400 km<sup>2</sup>. Xiangjiaba Hydropower Station is the last hydropower station in the development of cascade reservoirs on the lower reaches of the Jinsha River, it is 157 km away from the Xiluodu Hydropower Station, and its catchment area is 458,800 km<sup>2</sup>. Three Gorges is located in the middle of the Yangtze River, and the catchment area of the upper Yangtze River Basin (from headstream to TGP) is about 1,000,000 km<sup>2</sup>. The main characteristics of Xiluodu, Xiangjiaba, and Three Gorges are shown in Table 1.

**Table 1.** Main characteristics of Xiluodu, Xiangjiaba, and Three Gorges.

Reservoir Name	Normal Water Level (m)	Flood Control Limit Level (m)	Dead Water Level (m)	Firm Power Output (MW)	Installation Capacity (MW)
Xiluodu	600	560	560	3395	13,860
Xiangjiaba	380	370	370	2009	6000
Three Gorges	175	145	145	4990	22,400

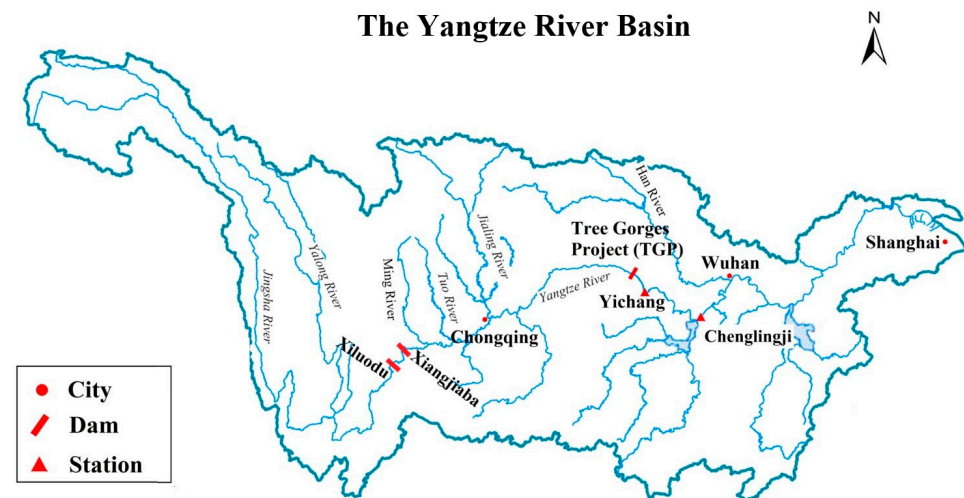


**Figure 5.** Location of Xiluodu, Xiangjiaba, and Three Gorges in the Yangtze River basin.

The flood control objective of Xiluodu–Xiangjiaba cascade reservoirs during the flood season is mainly divided into the following two parts: one is to ensure the safety of the flood control of Yibin, Luzhou, and Chongqing; the second is to cooperate with the Three Gorges Reservoir to intercept flood peaks in the middle and lower reaches of the Yangtze River to ensure the safety of Shashi and Chenglingji. The flood control objective of Three Gorges is to minimize the flood peaks for downstream areas (Shashi and Chenglingji) and control dam water levels to prevent potential major floods and ensure dam safety. The navigation objective of Three Gorges is to improve the navigability of ships of various powers to avoid ship grounding.

The historical daily flood data from June to September during the 41-year flood season from 1970 to 2010 are used. The one-day-ahead streamflow probability forecast result of the Xiluodu and Xiangjiaba cascade reservoirs and the three-day-ahead streamflow probability forecast result of Three Gorges are also used as the model input data. The water level of each reservoir at the beginning of the operation period is set as the flood limit water level.

### 3.2. Encoding and Constraints

#### 3.2.1. Individual Encoding

The RSEA is applied to the many-objective HPFOR optimization model of the Xiluodu, Xiangjiaba, and Three Gorges cascade reservoirs. According to the historical inflow and the downstream flood control standards of the Xiluodu, Xiangjiaba, and Three Gorges cascade reservoirs, the flow level of Xiluodu is divided into [0, 7500], [7500, 12,000], [12,000, 20,000], and [20,000, 25,000], the flow level of Xiangjiaba is divided into [0, 6500], [6500, 12,000], [12,000, 20,000], and [20,000, 25,000], and the flow level of Three Gorges is divided into [0, 30,000], [30,000, 40,000], [40,000, 45,000], [45,000, 50,000], and [50,000, 55,000]. The corresponding flow thresholds under each flow level  $x_1 \sim x_{13}$  and the flood retention flow of Xiluodu and Xiangjiaba  $x_{14}$  and  $x_{15}$  are encoded as decision variables, where the decision vector for each individual is represented as  $X = [x_1, x_2, \dots, x_{15}]$ .

#### 3.2.2. Constraint Handling

The constraints of the HPFOR optimization model can be divided into two categories including rigid constraints and flexible constraints. For rigid constraints such as the water balance constraint, storage volumes constraint, release constraint, and decision variables constraint, the program checks whether the constraints are satisfied during the evolutionary update process and dynamically modifies the decision variables to make them always meet the constraints. For flexible constraints such as output constraints, we define a constraint violation function and finitely select individuals with smaller constraint violation values during the evolutionary update process.

### 3.3. Results and Discussion

#### 3.3.1. Algorithm Performance Analysis

In order to analyze the performance of the RSEA on the many-objective optimization model of the HPFOR, three state-of-the-art algorithms, including MOEA/D, NSGA-III, and  $\theta$ -DEA, are also applied to the proposed many-objective optimization model for comparison. The systematic method proposed in the literature [41] is used to generate 85 weight vectors. The population size of the RSEA is set to 85, the neighborhood size is set to 20, the probability  $\delta$  is set to 0.9, the mutation probability is set to  $1/85$ , the variation distribution index is set to 20, and the maximum evolutionary generation of the algorithm is set to 500. The details of the parameter settings of the four algorithms are shown in Table 2.

**Table 2.** Parameter settings for the different algorithms.

Parameters	RSEA	MOEA/D	NSGA-III	$\theta$ -DEA
population size $N$	85	85	86	86
neighborhood size $T$	20	20	-	-
penalty parameter $\theta$	-	5	-	5
crossover probability $p_c$	-	1.0	1.0	1.0
crossover distribution index $\eta_c$	-	30	30	30
mutation probability $p_m$	$1/n$	$1/n$	$1/n$	$1/n$
mutation distribution index $\eta_m$	20	20	20	20

The hypervolume (HV) value is used in our study as the performance metric, which can simultaneously measure the convergence and diversity of the solution set. The HV metric value is defined as:

$$HV(\mathbf{S}, \mathbf{r}) = \text{volume} \left( \bigcup_{\mathbf{f} \in \mathbf{S}} [f_1, r_1] \times \dots \times [f_m, r_m] \right) \quad (26)$$

where  $\mathbf{S}$  is the set of final nondominated points;  $\mathbf{r} = (r_1, r_2, \dots, r_m)^T$  is a set of reference points in the objective space that is set to 1.1 times the upper bounds of the true Pareto front; and  $\text{volume}(\cdot)$  is the volume of the objective space dominated by the solutions in  $\mathbf{S}$  and bounded by  $\mathbf{r}$ . A larger HV value implies a better quality.

The average HV values of the MOEA/D, NSGA-III,  $\theta$ -DEA, and RSEA are presented in Table 3. The table shows that the HV value of the RSEA is the largest among the four algorithms, which verifies that the RSEA outperforms the other algorithms in both convergence and diversity. To see the convergence and diversity of different algorithms more intuitively, Figure 6 shows the radar figures of the final solution set obtained by the MOEA/D, NSGA-III,  $\theta$ -DEA, and RSEA. In the figure, all objectives are transformed into the maximum optimal objective so that the closer the solution in the radar graph is to the periphery, the better the objective value is. It can be seen from the radar figures that the final solution set of the MOEA/D is only distributed in a small part of the coordinate system, which indicates that the diversity of the MOEA/D is worse than the other algorithms. In terms of the diversity of the final solution set, the RSEA has the best distribution among the four algorithms. In terms of algorithm convergence, the MOEA/D only converges on the flood control station security objective, the objectives of the NSGA-III converged well except the power generation objective, and the  $\theta$ -DEA and RSEA perform better than the NSGA-III. The experimental results demonstrate that the RSEA can generally balance convergence and diversity well and outperform the other algorithms in the proposed many-objective optimization model.

**Table 3.** The average HV values of the MOEA/D, NSGA-III,  $\theta$ -DEA, and RSEA.

Algorithm	HV Value
MOEA/D	1.02782
NSGA-III	1.37412
$\theta$ -DEA	1.43363
RSEA	1.44494

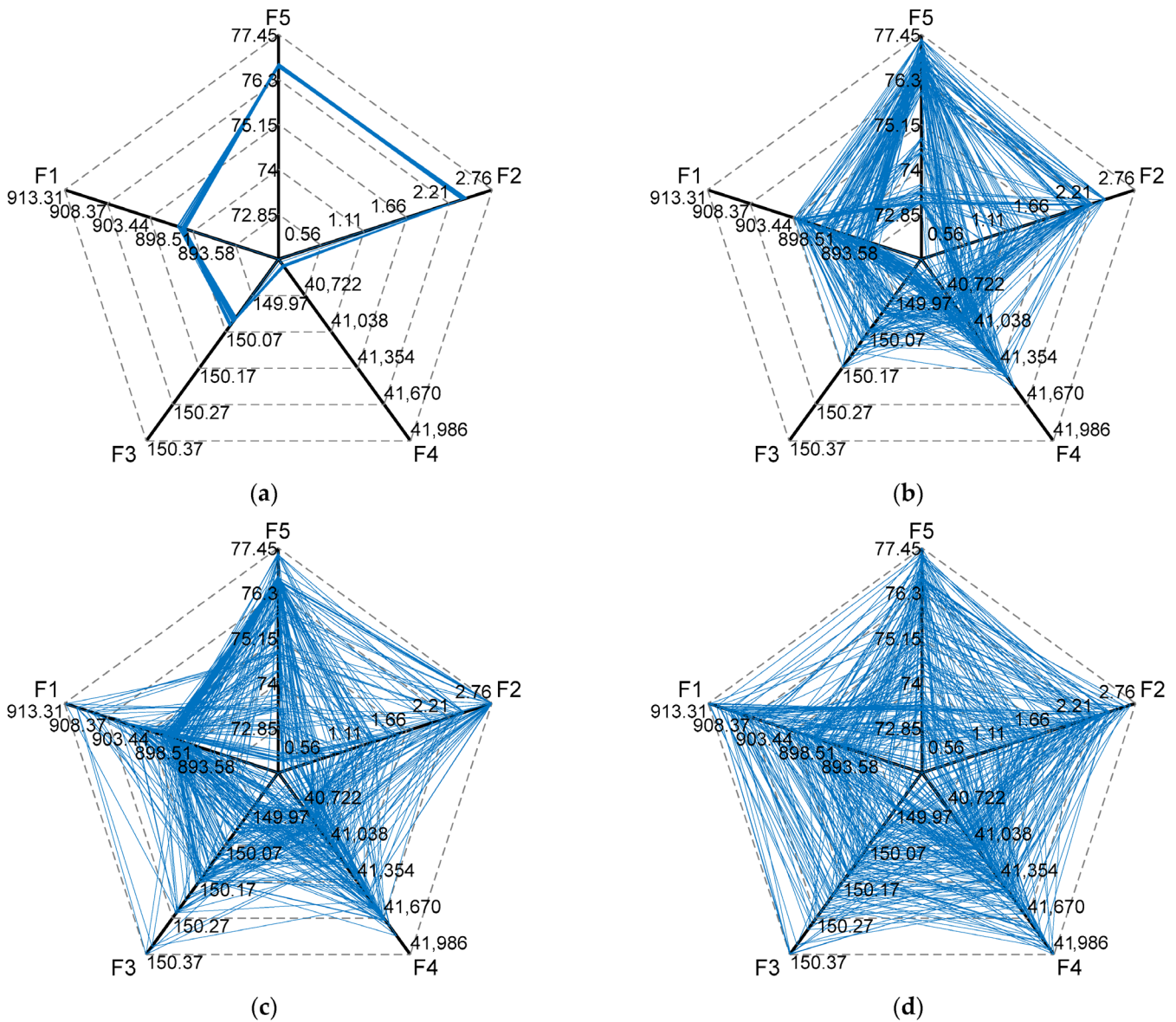


**Figure 6.** Radar figures of the final solution set obtained by MOEA/D, NSGAIII,  $\theta$ -DEA, and RSEA (F1: power generation objective, F2: reservoir safety objective, F3: flood control station security objective, F4: upstream cascade reservoirs flood control objective, F5: navigation objective). (a) MOEA/D, (b) NSGA-III, (c)  $\theta$ -DEA, and (d) RSEA.

### 3.3.2. Operation Process Analysis

Table 4 shows the final solution set of the flood operation rule obtained by the RSEA and lists the power generation objective, the flood control objective of the Xiluodu and Xiangjiaba cascade reservoirs, the flood control objective of Three Gorges, and the navigation objective for each solution. In addition, the operation result of the conventional flood control rule for the Xiluodu, Xiangjiaba, and Three Gorges cascade reservoirs is listed in

the first column of the table. All schemes satisfy the flood control constraints: the maximum water level of Three Gorges is lower than 171 m, and the maximum release flow of Three Gorges is less than  $5.5 \times 10^4 \text{ m}^3/\text{s}$ .

**Table 4.** The final solution set of the flood operation rule obtained by the RSEA.

N	F1 ( $10^8 \text{ kWh}$ )	F2 (m)	F3 ( $\text{m}^3/\text{s}$ )	F4 ( $10^8 \text{ m}^3$ )	F5 (%)	N	F1 ( $10^8 \text{ kWh}$ )	F2 (m)	F3 ( $\text{m}^3/\text{s}$ )	F4 ( $10^8 \text{ m}^3$ )	F5 (%)
-	885.56	149.95	41,132	1.97	77.44	43	901.23	150.02	41,006	0.75	74.92
1	913.31	150.28	41,297	2.31	73.32	44	901.23	150.04	40,903	1.15	75.11
2	913.14	150.29	41,325	2.28	73.30	45	901.22	150.02	40,804	2.12	75.69
3	912.35	150.37	41,411	0.98	73.33	46	901.00	150.01	41,074	1.47	74.69
4	912.35	150.37	41,413	0.96	73.34	47	900.92	149.98	40,782	2.51	75.98
5	912.04	150.25	41,314	2.09	73.39	48	900.85	150.09	40,840	1.90	74.18
6	911.96	150.27	41,549	0.70	73.30	49	900.73	150.07	40,544	2.39	75.42
7	911.40	150.34	41,566	0.87	73.36	50	900.57	150.10	41,362	0.01	72.64
8	911.13	150.21	41,382	1.96	73.44	51	900.46	150.08	41,218	0.74	76.29
9	910.85	150.22	41,089	2.33	72.58	52	899.58	150.08	40,634	2.43	76.66
10	910.79	150.30	41,625	0.21	73.32	53	899.57	150.06	40,482	2.43	76.68
11	910.58	150.17	41,440	0.69	73.43	54	899.50	150.05	40,475	2.43	76.68
12	910.17	150.23	41,130	1.79	72.49	55	899.49	150.05	40,572	2.43	76.68
13	910.12	150.24	41,215	1.54	72.47	56	899.26	149.96	41,065	1.36	75.01
14	909.76	150.21	41,875	0.19	73.42	57	899.08	149.96	40,936	2.40	75.16
15	909.55	150.25	41,636	0.92	73.43	58	898.46	150.04	40,621	2.42	76.63
16	909.04	150.19	41,424	0.48	72.85	59	898.03	150.11	40,716	1.93	76.50
17	908.69	150.16	41,094	2.63	73.78	60	897.90	149.96	41,419	1.26	75.54
18	908.67	150.20	41,713	0.50	73.53	61	897.77	149.94	41,052	2.70	76.31
19	907.97	150.21	41,839	0.13	73.52	62	897.69	149.94	41,028	2.55	76.33
20	907.66	150.15	41,051	2.63	73.92	63	897.62	149.95	41,476	1.48	75.48
21	907.13	150.11	41,428	2.05	72.79	64	897.57	150.02	41,336	0.05	74.65
22	907.01	150.15	41,176	1.70	71.81	65	897.41	149.97	41,454	1.54	75.84
23	906.99	150.20	41,539	0.98	73.67	66	896.98	150.00	41,004	1.38	76.53
24	906.58	150.14	41,791	0.38	72.23	67	896.76	150.00	41,516	0.58	74.88
25	906.12	150.15	41,298	1.36	71.70	68	896.60	149.97	41,196	1.17	76.01
26	905.58	150.11	41,275	1.58	71.92	69	896.42	149.87	40,828	2.28	75.25
27	905.07	150.12	41,180	2.15	73.05	70	896.16	150.00	41,233	0.53	76.76
28	904.53	150.16	41,933	0.30	72.86	71	895.93	149.94	41,353	2.12	77.14
29	904.48	150.13	41,986	0.28	72.85	72	895.36	149.97	41,255	0.51	76.98
30	904.39	150.12	41,957	0.40	72.72	73	895.02	149.96	41,447	0.40	77.45
31	903.98	150.07	41,164	1.87	73.06	74	894.97	149.89	40,931	2.01	75.30
32	903.97	150.07	41,129	1.62	72.01	75	894.90	150.03	41,261	0.46	76.66
33	903.54	150.12	41,584	1.05	73.47	76	894.37	149.88	40,776	2.29	77.18
34	903.12	150.09	41,063	1.33	74.38	77	893.85	149.91	40,872	2.39	77.23
35	903.11	150.18	41,590	0.24	73.56	78	892.55	149.95	41,216	1.08	76.94
36	903.05	150.14	41,853	0.57	73.86	79	892.49	149.98	41,423	0.24	76.92
37	902.52	150.08	40,970	1.51	74.23	80	892.20	149.90	40,922	2.21	77.31
38	902.41	150.15	41,776	0.76	73.21	81	891.19	149.96	41,083	1.34	77.26
39	902.23	150.02	40,817	2.12	74.53	82	890.69	149.92	40,875	1.90	76.60
40	901.94	150.10	41,054	1.27	74.36	83	889.73	149.92	40,982	1.18	77.33
41	901.93	150.12	41,495	0.07	72.56	84	889.56	149.94	41,171	0.28	77.35
42	901.61	150.03	41,060	1.62	74.58	85	888.65	149.94	41,389	0.22	77.29

It can be seen from the table that the average multi-year power generation of the cascade reservoirs is  $885.59 \times 10^8 \text{ kWh}$  under the conventional flood control rule and between  $888.65 \times 10^8 \text{ kWh}$  and  $913.31 \times 10^8 \text{ kWh}$  under the optimal HPFORs, which can increase the power generation benefit by a maximum of  $27.72 \times 10^8 \text{ kWh}$ . The multi-year average maximum flood control level of Three Gorges is 149.95 m under the conventional flood control rule and between 149.87 m and 150.37 m under the optimal HPFORs. The multi-year average maximum release flow of Three Gorges is  $41,132 \text{ m}^3/\text{s}$  under the con-

ventional flood control rule and between 40,475 m<sup>3</sup>/s and 41,986 m<sup>3</sup>/s under the optimal HPFORs. The usage of the Xiluodu–Xiangjiaba cascade flood control storage capacity is 1.97 × 10<sup>8</sup> m<sup>3</sup> under the conventional flood control rule and between 0.01 × 10<sup>8</sup> m<sup>3</sup> and 2.70 × 10<sup>8</sup> m<sup>3</sup> under the optimal HPFORs. The navigation rate of Three Gorges is 77.44% under the conventional flood control rule and between 71.70% and 77.35% under the optimal HPFORs. These data indicate that the proposed optimal HPFORs can significantly improve the power generation efficiency of cascade reservoirs without overly affecting flood control and navigation objectives.

In order to further analyze the real-time flood operation process of cascade reservoirs, four typical schemes including 1, 25, 57, and 85 are chosen for verification. Figures 7 and 8 show the flow processes and water level processes of Three Gorges under the simulation of four typical schemes of the conventional flood control rule in 1981 and 1998, respectively. From the figures, we can see that the main differences between the proposed optimal HPFOR and the conventional flood control rule are the following: (1) When the current inflow is small and the forecast inflow is less than the flow threshold in the future, the reservoir will store water according to the HPFOR, while the reservoir remains at the flood limit level under the conventional flood control rule. (2) When the current inflow is small and the forecast inflow is larger than the flow threshold in the future, the reservoir will pre-release according to the HPFOR to ensure flood control safety. (3) During the flood recession period, the reservoir will quickly empty the storage capacity through the limit of the discharge flow under the conventional flood control rule, while the HPFOR will gradually reduce the reservoir water level according to the forecast inflow.

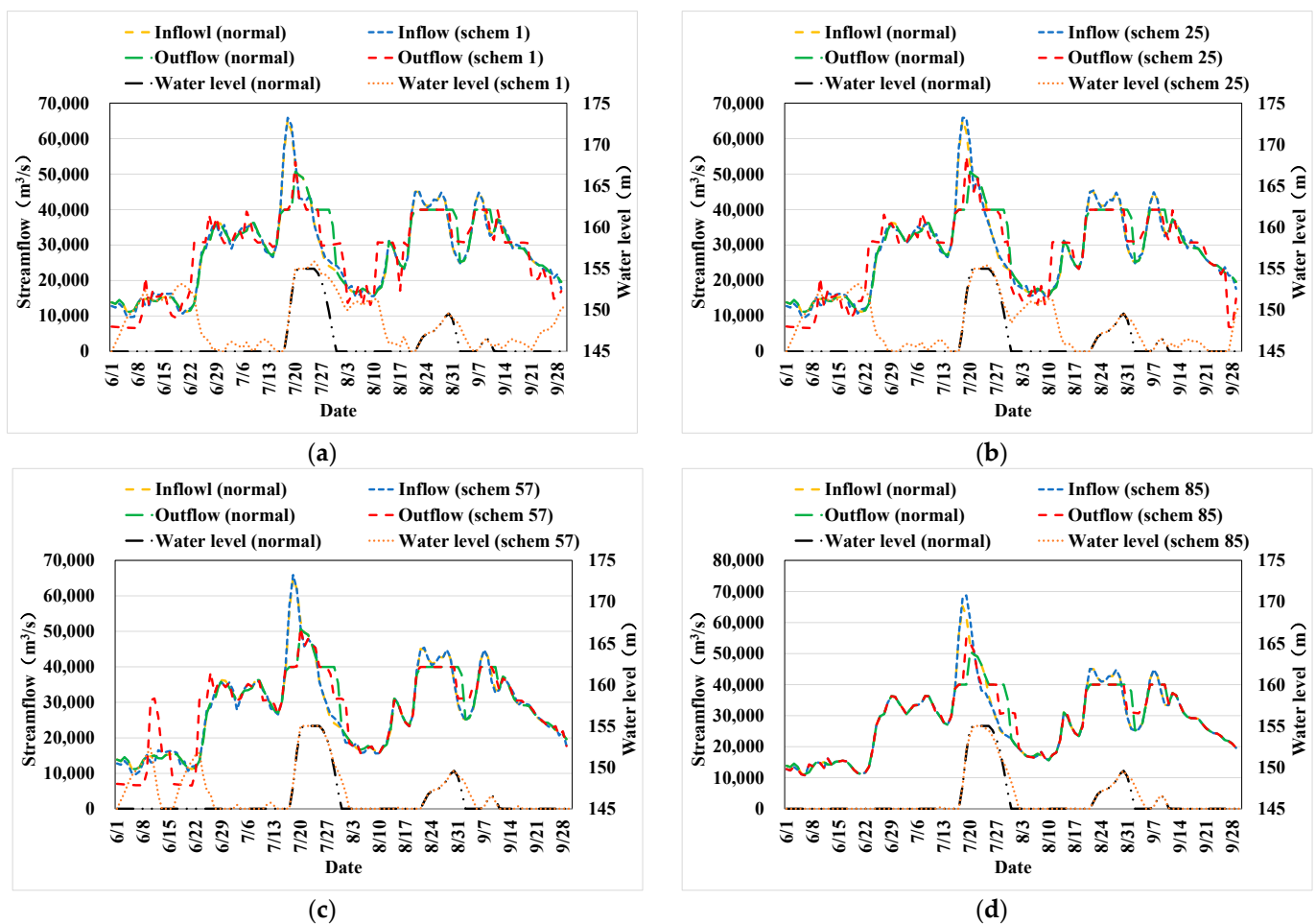
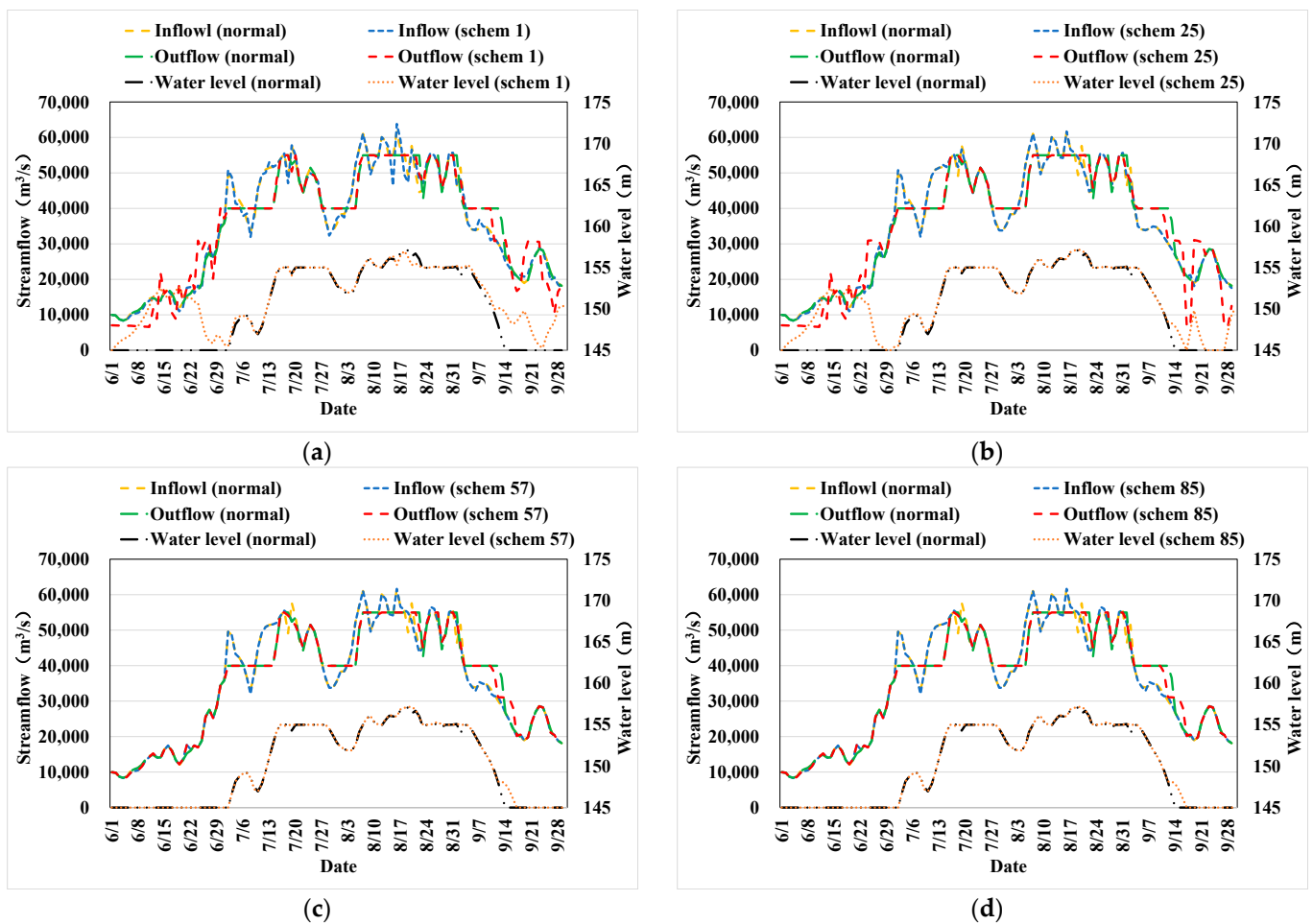


Figure 7. Release processes and water level processes of Three Gorges in 1981: (a) scheme 1, (b) scheme 25, (c) scheme 57, and (d) scheme 85.



**Figure 8.** Release processes and water level processes of Three Gorges in 1998: (a) scheme 1, (b) scheme 25, (c) scheme 57, and (d) scheme 85.

The four typical schemes 1, 25, 57, and 85 have different hierarchical flow thresholds, resulting in differences in pre-fill and pre-release processes. It can be seen from the figure that scheme 1 executes pre-fill processes when the inflow is small, which can raise the power generation head to increase power generation efficiency. Scheme 1 also executes pre-release processes, which can reduce the water level to the flood limit level before the flood to ensure the safety of subsequent flood control. The release and water level processes of scheme 85 are closest to the conventional flood control rule. This is because the flow threshold of scheme 85 is close to the lower boundary of the flow level, which will reduce the frequency of pre-fill processes. The only difference between scheme 85 and the conventional flood control rule is the pre-release processes during the flood recession period. Scheme 85 slows down the rate of water level decline, which can reduce the water abandonment of the reservoir.

In summary, the proposed HPFOR can effectively utilize future streamflow forecast and its uncertainty information and use the hierarchical pre-fill and pre-release strategy to instruct the reservoir pre-fill and pre-release operations. The simulation operation results indicate that the HPFOR can improve the water volume and head efficiency of cascade reservoirs under the condition of flood control safety, which is beneficial for the utilization of small and medium flood resources.

### 3.3.3. Comparison with Other Studies

The comparison of the RSEA with other state-of-the-art algorithms demonstrates that the RSEA can balance convergence and diversity well and outperform other algorithms

when applied to the many-objective optimization model of the HPFOR. The comparison of optimal HPFORs with the conventional flood control rule indicates that the HPFOR can significantly improve power generation under the condition of flood control safety. In addition to the comparison with other algorithms and the conventional flood control rule, a recent hierarchical flood operation rule (HFOR) for the utilization of small and medium flood resources is reproduced and compared to the HPFOR in this section.

The water level processes of Three Gorges in 1981 and 1998 of the HFOR, HPFOR, and conventional flood control rule are shown in Figure 9. From the figure, we can see that the water level of the HFOR remains at the flood limit water level 145 m before the flood, which is the same as the conventional flood control rule. However, when a large flood occurs, the HFOR controls the outflow of Three Gorges based on the water level and inflow, causing the water level to rise rapidly to around 165 m, increasing future flood control risks. In contrast, the HPFOR raises the operating water level of Three Gorges to around 153 m when the inflow is small and pre-releases before the large flood comes, reducing the water level to 145 m without increasing the flood control risks downstream. When a large flood occurs, Three Gorges operates at the flood limit level of 145 m. This result indicates that the HFOR improves water resource utilization by using graded outflow but increases flood risks, while the HPFOR improves the utilization of small and medium floods and reduces flood control risks of large floods by utilizing forecast information, which provides safer and more reliable decision-making information for the reservoir managers.

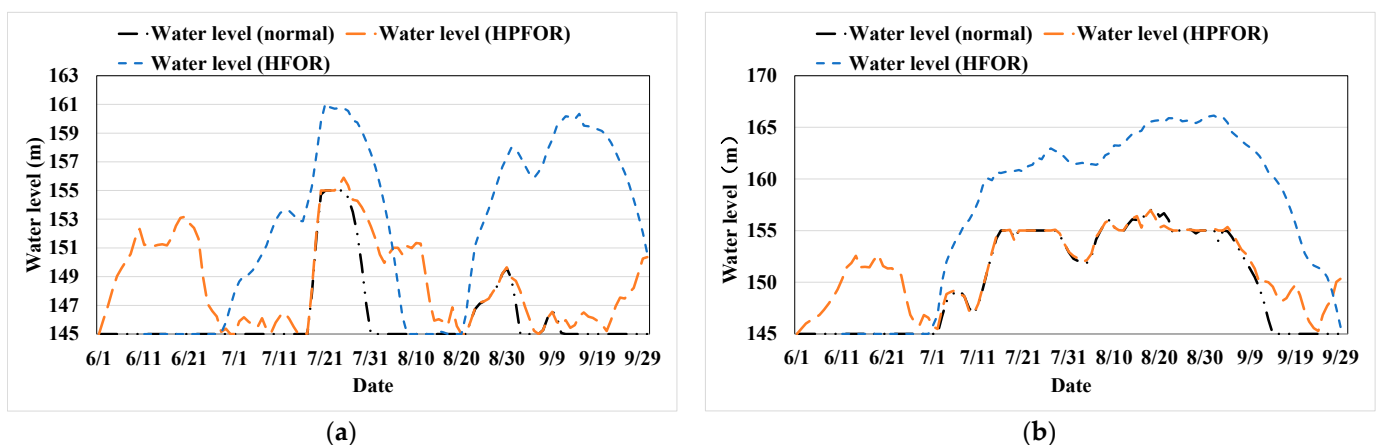


**Figure 9.** Water level processes of Three Gorges in 1981 and 1998: (a) 1981 and (b) 1998.

#### 4. Conclusions

In this paper, the HPFOR, which is based on the two-stage reservoir operation model and streamflow forecast uncertainty information, is proposed for cascade reservoir flood control. Moreover, the many-objective optimization model of the HPFOR is established, and the RSEA is employed to optimize the many-objective model. According to the experimental results, we can find that the optimal HPFORs can execute the reservoir pre-fill and pre-release operations at appropriate times and significantly improve the power generation efficiency of a cascade reservoir without overly affecting flood control and navigation.

This study develops a novel flood control rule, a hierarchical pre-release flood control rule, which utilizes the small and medium flood resources through flood forecasting and its uncertainty information. A many-objective optimization model is proposed by parameterizing the proposed flood control rule, and the region search evolutionary algorithm is employed to optimize the many-objective model. Then, the proposed model is applied in a real-world case study upstream of the Yangtze River basin. The optimization experimental results are compared with three state-of-the-art algorithms, and the results show that the region search evolutionary algorithm can balance convergence and diversity well and outperform the other algorithms in the proposed many-objective optimization

model. The simulation operation results of cascade reservoirs are also shown, indicating that the optimized flood rule can improve the water volume and head efficiency of cascade reservoirs under the condition of flood control safety, which is beneficial for the utilization of small and medium flood resources. In summary, the real-world case study shows that the proposed hierarchical pre-release flood control rule can use flood forecast information to improve the utilization of small and medium floods and reduce the flood control risk of large floods, which can provide a reliable decision direction for dispatch managers.

**Author Contributions:** Conceptualization, Y.L.; Methodology, Y.L.; Software, Y.L.; Validation, R.T.; Formal analysis, Y.L. and B.W.; Investigation, G.H.; Resources, Y.L. and G.H.; Data curation, Y.L. and T.W.; Writing—original draft, Y.L.; Writing—review & editing, H.Q.; Supervision, B.W. and Y.X.; Project administration, B.W. and Y.X.; Funding acquisition, Y.X. All authors have read and agreed to the published version of the manuscript.

**Funding:** This research was funded by National Key Research and Development Program of China, grant number 2021YFC3200303; and Open Research Fund of Hubei Key Laboratory of Intelligent Yangtze and Hydroelectric Science, China Yangtze Power Co., Ltd., grant number ZH2102000110; and National Natural Science Foundation of China, grant number 51979113.

**Data Availability Statement:** The data presented in this study are available on request from the corresponding author. The data are not publicly available due to data confidentiality issues.

**Conflicts of Interest:** Author Y.L. was employed by the company China Water Resources Pearl River Planning Surveying & Designing Co., Ltd. The remaining authors declare that the research was conducted in the absence of any commercial or financial relationships that could be construed as a potential conflict of interest.

## References

1. Towfiqul Islam, A.R.M.; Talukdar, S.; Mahato, S.; Kundu, S.; Eibek, K.U.; Pham, Q.B.; Kuriqi, A.; Thuy Linh, N.T. Flood susceptibility modelling using advanced ensemble machine learning models. *Geosci. Front.* **2021**, *12*, 101075. [[CrossRef](#)]
2. Costache, R. Flash-flood Potential Index mapping using weights of evidence, decision Trees models and their novel hybrid integration. *Stoch. Environ. Res. Risk Assess.* **2019**, *33*, 1375–1402. [[CrossRef](#)]
3. Alexander, K.; Hettiarachchi, S.; Ou, Y.; Sharma, A. Can integrated green spaces and storage facilities absorb the increased risk of flooding due to climate change in developed urban environments? *J. Hydrol.* **2019**, *579*, 124201. [[CrossRef](#)]
4. Xu, L.; Wang, X.; Liu, J.; He, Y.; Tang, J.; Nguyen, M.; Cui, S. Identifying the trade-offs between climate change mitigation and adaptation in urban land use planning: An empirical study in a coastal city. *Environ. Int.* **2019**, *133*, 105162. [[CrossRef](#)]
5. Pan, Z.; Chen, L.; Teng, X. Research on joint flood control operation rule of parallel reservoir group based on aggregation–decomposition method. *J. Hydrol.* **2020**, *590*, 125479. [[CrossRef](#)]
6. Oliveira, R.; Loucks, D.P. Operating rules for multireservoir systems. *Water Resour. Res.* **1997**, *33*, 839–852. [[CrossRef](#)]
7. Huang, A.; Gao, G.; Yao, L.; Yin, S.; Li, D.; Do, H.X.; Fu, B. Spatiotemporal variations of inter- and intra-annual extreme streamflow in the Yangtze River Basin. *J. Hydrol.* **2024**, *629*, 130634. [[CrossRef](#)]
8. Howard, R.A. Dynamic Programming. *Manag. Sci.* **1966**, *5*, 317–348. [[CrossRef](#)]
9. Deb, K.; Pratap, A.; Agarwal, S.; Meyarivan, T. A fast and elitist multiobjective genetic algorithm: NSGA-II. *IEEE Trans. Evol. Comput.* **2002**, *6*, 182–197. [[CrossRef](#)]
10. Huang, W.C.; Wu, C.M. Diagnostic Checking in Stochastic Dynamic Programming. *J. Water Resour. Plan. Manag.* **1993**, *119*, 490–494. [[CrossRef](#)]
11. Suiadee, W.; Tingsanchali, T. A combined simulation–genetic algorithm optimization model for optimal rule curves of a reservoir: A case study of the Nam Oon Irrigation Project, Thailand. *Hydrol. Process.* **2007**, *21*, 3211–3225. [[CrossRef](#)]
12. Yang, P.; Ng, T.L. Fuzzy Inference System for Robust Rule-Based Reservoir Operation under Nonstationary Inflows. *J. Water Resour. Plan. Manag.* **2017**, *143*, 04016084. [[CrossRef](#)]
13. Feng, Z.; Niu, W.; Zhang, R.; Wang, S.; Cheng, C. Operation rule derivation of hydropower reservoir by k-means clustering method and extreme learning machine based on particle swarm optimization. *J. Hydrol.* **2019**, *576*, 229–238. [[CrossRef](#)]
14. Liu, Y.; Qin, H.; Zhang, Z.; Yao, L.; Wang, Y.; Li, J.; Liu, G.; Zhou, J. Deriving reservoir operation rule based on Bayesian deep learning method considering multiple uncertainties. *J. Hydrol.* **2019**, *579*, 124207. [[CrossRef](#)]
15. Chen, L.; McPhee, J.; Yeh, W.W.G. A diversified multiobjective GA for optimizing reservoir rule curves. *Adv. Water Resour.* **2007**, *30*, 1082–1093. [[CrossRef](#)]
16. Chang, L.; Chang, F. Multi-objective evolutionary algorithm for operating parallel reservoir system. *J. Hydrol.* **2009**, *377*, 12–20. [[CrossRef](#)]
17. Gomes, M.D.G.; Maia, A.G.; Medeiros, J.D.F.D. Reservoir operation rule in semiarid areas: The quantity-quality approach. *J. Hydrol.* **2022**, *610*, 127944. [[CrossRef](#)]

18. Moeini, R.; Hadiyan, P.P. Hybrid methods for reservoir operation rule curve determination considering uncertain future condition. *Sustain. Comput. Inform. Syst.* **2022**, *35*, 100727. [[CrossRef](#)]
19. Jiang, Z.; Liu, P.; Ji, C.; Zhang, H.; Chen, Y. Ecological flow considered multi-objective storage energy operation chart optimization of large-scale mixed reservoirs. *J. Hydrol.* **2019**, *577*, 123949. [[CrossRef](#)]
20. Liu, Y.; Qin, H.; Mo, L.; Wang, Y.; Chen, D.; Pang, S.; Yin, X. Hierarchical Flood Operation Rules Optimization Using Multi-Objective Cultured Evolutionary Algorithm Based on Decomposition. *Water Resour. Manag.* **2019**, *33*, 337–354. [[CrossRef](#)]
21. Ahmadianfar, I.; Kheyrandish, A.; Jamei, M.; Gharabaghi, B. Optimizing operating rules for multi-reservoir hydropower generation systems: An adaptive hybrid differential evolution algorithm. *Renew. Energy* **2021**, *167*, 774–790. [[CrossRef](#)]
22. He, S.; Guo, S.; Zhang, J.; Liu, Z.; Cui, Z.; Zhang, Y.; Zheng, Y. Multi-objective operation of cascade reservoirs based on short-term ensemble streamflow prediction. *J. Hydrol.* **2022**, *610*, 127936. [[CrossRef](#)]
23. Bourdin, D.R.; Fleming, S.W.; Stull, R.B. Streamflow Modelling: A Primer on Applications, Approaches and Challenges. *Atmosphere-Ocean* **2012**, *50*, 507–536. [[CrossRef](#)]
24. Liu, Y.; Ye, L.; Qin, H.; Ouyang, S.; Zhang, Z.; Zhou, J. Middle and Long-Term Runoff Probabilistic Forecasting Based on Gaussian Mixture Regression. *Water Resour. Manag.* **2019**, *33*, 1785–1799. [[CrossRef](#)]
25. Wu, C.L.; Chau, K.W.; Li, Y.S. Predicting monthly streamflow using data-driven models coupled with data-preprocessing techniques. *Water Resour. Res.* **2009**, *45*, W08432. [[CrossRef](#)]
26. Ye, L.; Zhou, J.; Gupta, H.V.; Zhang, H.; Zeng, X.; Chen, L. Efficient estimation of flood forecast prediction intervals via single- and multi-objective versions of the LUBE method. *Hydrol. Process.* **2016**, *30*, 2703–2716. [[CrossRef](#)]
27. You, J.; Cai, X. Hedging rule for reservoir operations: 1. A theoretical analysis. *Water Resour. Res.* **2008**, *44*, W01415. [[CrossRef](#)]
28. You, J.; Cai, X. Hedging rule for reservoir operations: 2. A numerical model. *Water Resour. Res.* **2008**, *44*, W01416. [[CrossRef](#)]
29. Zhao, T.; Zhao, J.; Lund, J.R.; Yang, D. Optimal Hedging Rules for Reservoir Flood Operation from Forecast Uncertainties. *J. Water Resour. Plan. Manag.* **2014**, *140*, 04014041. [[CrossRef](#)]
30. Ding, W.; Zhang, C.; Peng, Y.; Zeng, R.; Zhou, H.; Cai, X. An analytical framework for flood water conservation considering forecast uncertainty and acceptable risk. *Water Resour. Res.* **2015**, *51*, 4702–4726. [[CrossRef](#)]
31. Tan, Q.; Wang, X.; Wang, H.; Wang, C.; Lei, X.H.; Xiong, Y.S.; Zhang, W. Derivation of optimal joint operating rules for multi-purpose multi-reservoir water-supply system. *J. Hydrol.* **2017**, *551*, 253–264. [[CrossRef](#)]
32. Mohammad Ashrafi, S. Two-Stage Metaheuristic Mixed Integer Nonlinear Programming Approach to Extract Optimum Hedging Rules for Multireservoir Systems. *J. Water Resour. Plan. Manag.* **2021**, *147*, 04021070. [[CrossRef](#)]
33. Liu, Y.; Hou, G.; Huang, F.; Qin, H.; Wang, B.; Yi, L. Directed graph deep neural network for multi-step daily streamflow forecasting. *J. Hydrol.* **2022**, *607*, 127515. [[CrossRef](#)]
34. Liu, Y.; Ye, L.; Qin, H.; Hong, X.; Ye, J.; Yin, X. Monthly streamflow forecasting based on hidden Markov model and Gaussian Mixture Regression. *J. Hydrol.* **2018**, *561*, 146–159. [[CrossRef](#)]
35. Liu, Y.; Qin, H.; Zhang, Z.; Yao, L.; Wang, C.; Mo, L.; Shuo, Q.; Jie, L. A region search evolutionary algorithm for many-objective optimization. *Inf. Sci.* **2019**, *488*, 19–40. [[CrossRef](#)]
36. Li, X.; Guo, S.; Liu, P.; Chen, G. Dynamic control of flood limited water level for reservoir operation by considering inflow uncertainty. *J. Hydrol.* **2010**, *391*, 124–132. [[CrossRef](#)]
37. Zhang, Q.; Li, H. MOEA/D: A Multiobjective Evolutionary Algorithm Based on Decomposition. *IEEE Trans. Evol. Comput.* **2007**, *11*, 712–731. [[CrossRef](#)]
38. Deb, K.; Jain, H. An Evolutionary Many-Objective Optimization Algorithm Using Reference-Point-Based Nondominated Sorting Approach, Part I: Solving Problems With Box Constraints. *IEEE Trans. Evol. Comput.* **2014**, *18*, 577–601. [[CrossRef](#)]
39. Yuan, Y.; Xu, H.; Wang, B.; Yao, X. A New Dominance Relation-Based Evolutionary Algorithm for Many-Objective Optimization. *IEEE Trans. Evol. Comput.* **2016**, *20*, 16–37. [[CrossRef](#)]
40. Liu, Y.; Zhan, X.; Lyu, H.; Qin, H. Region search evolutionary algorithm with constraint handling for multi-objective short-term wind-solar-hydro-thermal scheduling. *E3S Web Conf.* **2021**, *233*, 01018. [[CrossRef](#)]
41. Li, K.; Deb, K.; Zhang, Q.; Kwong, S. An Evolutionary Many-Objective Optimization Algorithm Based on Dominance and Decomposition. *IEEE Trans. Evol. Comput.* **2015**, *19*, 694–716. [[CrossRef](#)]

**Disclaimer/Publisher’s Note:** The statements, opinions and data contained in all publications are solely those of the individual author(s) and contributor(s) and not of MDPI and/or the editor(s). MDPI and/or the editor(s) disclaim responsibility for any injury to people or property resulting from any ideas, methods, instructions or products referred to in the content.